*vibration*

MDPI

*Article*

# Numerical and Experimental Study of Structural Parameter Identification for Jacket-Type Offshore Wind Turbines

**Xu Han [1,2,*], Chen Zhang [3], Zhaoyang Guo [1], Wenhua Wang [1,2], Qiang Liu [4] and Xin Li [1,2]**

[1] School of Infrastructure Engineering, Dalian University of Technology, Dalian 116024, China; guozhaoyang@mail.dlut.edu.cn (Z.G.); whwanghydro@dlut.edu.cn (W.W.); lixin@dlut.edu.cn (X.L.)
[2] Ningbo Key Laboratory of Integrated Development and Safety Assurance for Deep-Sea Energy and Resources, Ningbo Institute of Dalian University of Technology, Ningbo 315016, China
[3] China Nuclear Power Engineering Co., Ltd., Beijing 100840, China
[4] PowerChina Huadong Engineering Corporation Limited, Hangzhou 311122, China; liu_q@hdec.com
* Correspondence: xu.han@dlut.edu.cn

## Abstract

Offshore wind energy has developed rapidly in recent years as a crucial component of renewable energy. However, offshore wind turbines (OWTs) face significant challenges in operations under complex marine environmental conditions, such as multimodal nonlinear vibrations, reliable structural monitoring, efficient maintenance, and sustainable long-term operations. The model-updating-based parameter identification takes advantages of structural vibration measurements, assisting in structural health monitoring. However, the traditional methods have not fully accounted for the parameter uncertainties and the need for real-time state updating, making them insufficient to meet the long-term online monitoring requirements for OWTs. This study introduces an innovative structural parameter identification framework that integrates modal parameter identification with Bayesian recursive updating. The proposed framework enables more efficient updates and uncertainty quantification of critical physical parameters for OWTs. It combines the covariance-driven stochastic subspace identification (COV-SSI) method for automatic modal parameter identification with the unscented Kalman filter (UKF) for parameter estimation. A 10 MW jacket-type offshore wind turbine was used as a case study. First, the numerical simulations were conducted to generate synthetic measurements for method validation and demonstration, enabling stepwise updating of the tower material's elastic modulus across different sea conditions. A comparison of update speed and the convergence rate with the traditional time-step-based UKF method demonstrated the superiority of the proposed sea-condition-based approach in terms of computational efficiency and stability. Finally, the proposed framework was systematically validated using scaled model experimental data of a jacket-type OWT with a 4.2% identification error, confirming its engineering applicability. This research provides reliable technical support for the safety assessment of offshore wind turbine structures.

**Keywords:** jacket-type foundation; offshore wind turbine; unscented Kalman filter; parameter identification

Check for updates

Academic Editors: Aleksandar Pavic and Alhussein Albarbar

Received: 11 February 2026
Revised: 14 March 2026
Accepted: 9 April 2026
Published: 14 April 2026

**Copyright:** © 2026 by the authors. Licensee MDPI, Basel, Switzerland. This article is an open access article distributed under the terms and conditions of the Creative Commons Attribution (CC BY) license.

## 1. Introduction

With continuous advancements in offshore engineering, offshore wind energy offers notable advantages, such as higher wind speeds and more stable power output, making it one of the fastest-growing renewable energy sources [1]. However, compared to land-based

environments, offshore wind turbines operate in harsher environmental conditions. They are subjected to long-term cyclic vibrating loads from wind, waves, currents, etc. They may also experience extreme events like typhoons and earthquakes. These complex multimodal nonlinear vibrations could further lead to operational risks. Consequently, the operational safety of offshore wind turbines has attracted considerable attention from industries and academics.

Digital twin technology holds great potential in the field of marine structural health monitoring and risk assessment. High-fidelity and accurate numerical models play a crucial role in assessing the safety of OWTs. Sensing the changes in critical structural parameters and updating them correctly in time is important for the digital twin system [2]. The structural dynamic system identification methods can effectively obtain the key parameters for structural condition assessments. The commonly used system identification methods in structural health monitoring include modal parameter identification and physics-based model updating methods. The modal parameters (including natural frequency, damping ratio, and mode shapes) effectively reflect the dynamic characteristics of structures. Their accurate identification provides essential data for structural damage detection and condition assessment [3]. Operational modal analysis (OMA) is a widely applied category of modal parameter identification methods for OWTs that requires only output data and does not need the input conditions to be known [4–7]. It usually analyzes the structural vibration signals to identify the modal parameters, which play a crucial role in health monitoring and damage identification during the operation and maintenance of structures. However, the OMA techniques have certain limitations. The loads on OWTs are strongly coupled with the physical properties of the structure, and the operating states are more complex [8]. Consequently, the modal parameters alone cannot fully assess the structural safety. In addition to the modal parameters, changes in the parameters, such as stiffness and mass, also affect the distribution of the strain field in the structure [9]. These parameters play a key role in damage and fatigue assessments. The parameter identification method based on finite element model updating allows for the precise identification of key physical parameters by iteratively updating unknown parameters through an inverse process [10].

Model updating typically employs deterministic optimization strategies, aiming to minimize the deviation between the predicted and the measured responses. However, this kind of updating process is not able to quantify parameter uncertainty and struggles to obtain global optima. For OWTs, physical parameters such as soil stiffness, corrosion, marine biofouling, hub mass, and nacelle stiffness exhibit significant uncertainties. They consequently affect numerical modeling in terms of pile stiffness, soil stiffness, added mass, drag, and connection stiffness [6]. Most physics-based parameter identification methods based on model updating are founded on linear assumptions. However, OWTs often exhibit significant nonlinearity and uncertainty when operating in complex marine environments. The traditional deterministic methods struggle to handle such issues effectively. On the other hand, the Bayesian statistical inference methods, by integrating prior knowledge (such as engineering experience or historical data) with field monitoring data, establish posterior probability distributions for parameters [11]. Applying the Bayesian theory to model parameter updating also helps quantify parameter uncertainty, thus improving the rationality of identification [12].

Bayesian model updating can be divided into two approaches: batch processing and recursive processing. In the batch processing mode, the system integrates all available monitoring data to establish a likelihood function, from which the posterior distribution of parameters is derived [13–18]. The Bayesian batch processing methods have made significant achievements in the field of monopile offshore wind turbines. For instance, Xu et al. [19] proposed a novel Bayesian updating framework integrating the Transition

Markov Chain Monte Carlo. A function based on measured natural frequency and damping ratio was established to update the soil-structure stiffness and damping for offshore wind turbines, hereby quantifying the uncertainty and providing a significant engineering value to Bayesian model updating. Moynihan et al. [20] applied the Bayesian updating methods to successfully invert the posterior probability distribution of soil-structure stiffness using field-measured data for a 6 MW monopile offshore wind turbine. The uncertainty quantification for the key parameters was realized, providing a reference for the application of probabilistic assessment methods in offshore wind turbine health monitoring.

Compared to the batch processing methods, the recursive Bayesian methods have the advantage of real-time processing. These methods dynamically update the state by integrating the latest measurements and generating a series of posterior distributions at different time steps. The common recursive Bayesian methods include Kalman filtering (KF) and its extended methods for nonlinear systems, such as particle filtering (PF) [21,22], extended Kalman filtering (EKF) [23,24], and unscented Kalman filtering (UKF) [25–27].

Significant progress has also been made in the synchronous identification of structural physical parameters and unknown loads. Song et al. [26] proposed an adaptive Kalman filtering method that simultaneously updates noise variance and model parameters, effectively alleviating the impact of modeling errors on parameter identification accuracy. To better address the damage identification problem of strongly nonlinear structures, Li et al. [28] developed a novel constrained UKF method achieving the synchronous identification of parameters and unknown seismic excitations for a three-story, three-span steel frame and a three-span continuous reinforced concrete bridge structure. Song et al. [29] proposed a joint physical parameter-input load estimation technique based on a windowed UKF method, which was applied to real offshore platform engineering practices. Later, Song et al. [30] introduced the windowing approach into the EKF method, using sparse measurements to estimate the physical parameters and dynamic input loads of offshore wind turbines. This offered essential technical support for the development of a digital twin system for offshore wind turbines. While the overlapping window approach enhances the accuracy of parameter identification, it simultaneously introduces data redundancy, thereby increasing the computational complexity. Compared to EKF, UKF demonstrates a superior performance in highly nonlinear scenarios with good convergence stability and high accuracy, eliminating the need for Jacobian matrix computation.

The traditional time-step-based Bayesian updating methods suffer from high computational complexity and slow convergence. This leads to challenges in parameter identification, accounting for coupling effects on marine structures. This severely limits the method's application in engineering. Compared to each time step, the dynamics of marine structures in a short period, defined as a sea condition (i.e., typically 10 min for wind and 0.5–3 h for waves), are stationary. The statistical presentation of dynamic responses is stable. Updating based on those short-term statistics within each sea condition could potentially require less computational effort. Han et al. [31] proposed a UKF-based ship seakeeping model parameter identification method using the observed response characteristics of a vessel under multiple sea states. Online updating and uncertainty quantification of key seakeeping parameters were achieved, significantly improving the computational efficiency.

Compared with monopile-supported OWTs, the jacket-type OWTs become a more cost-effective solution towards deeper and farther waters [32]. However, these bring challenges in terms of online monitoring and efficient operation. In addition, the structural complexity of the foundation could potentially lead to challenges in model updating. This study presents a sea-condition-based parameter identification method for jacket-type OWTs based on UKF. It uses the structural vibration signals to extract the modal parameters and further identify the physical parameters as the observation space. Using a 10 MW jacket-

type OWT as a case study, the method is validated by numerical simulations and scaled model test data. This study overcomes the limitations of the conventional time-step-based Bayesian recursive updating methods in terms of computational efficiency and engineering applicability, providing a novel technical pathway for offshore wind turbine digital twin systems.

The remainder of this paper is organized as follows: Section 2 introduces the theory of the proposed improved UKF for structural parameter identification. Section 3 describes the numerical model of the jacket-type offshore wind turbine. Section 4 analyzes the identification results under different operating conditions and discusses the influence of operating conditions on these results. Section 5 presents further validation based on the experimental data from scaled model tests. Finally, the conclusions are drawn in Section 6.

## 2. Methodology Description

The core idea of the sea-condition-based parameter identification method is to use the unscented transformation (UT) to propagate and update the state space based on prior knowledge and observations according to nonlinear relationships between the state and observation spaces. It selects a set of sample points to approximate the distribution of the state. By using a deterministic sampling strategy (sigma point sampling), UKF accurately captures the mean and covariance of the random variables after nonlinear transformations, avoiding the higher-order truncation errors that arise from the traditional Taylor expansion linearization. This approach provides a more accurate and stable solution to nonlinear problems. This method primarily involves three steps: sigma point sampling, state propagation, and measurement update. The flowchart of the proposed method is shown in Figure 1. Details of the method are described in the following subsections.

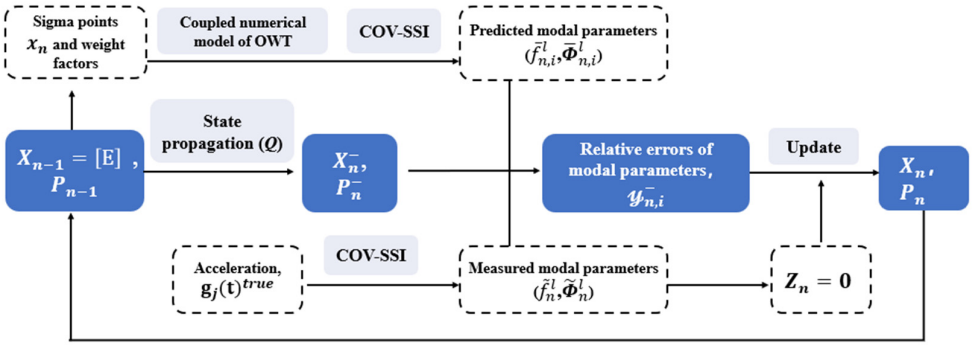



**Figure 1.** A flowchart of the proposed sea-condition-based parameter identification method.

### *2.1. Sigma Point Sampling*

In the proposed method, the state space ($\boldsymbol{X}$, $\boldsymbol{P}$) is first established. $\boldsymbol{X}$ is the state vector, including the key uncertain structural parameters to be updated. $\boldsymbol{P}$ is the state covariance matrix, representing the uncertainties of the state. The elastic modulus ($E$) reflects the structural stiffness variation to some extent, potentially indicating the level of structural damage [33]. Therefore, the elastic modulus of the tower was considered as the state $\boldsymbol{X}_{n-1}$ after the $(n-1)$-th update, with uncertainty of $\boldsymbol{P}_{n-1}$.

It is assumed that the state space (i.e., structural parameters) remains approximately unchanged for each sea condition defined by a combination of a stationary sea state (described by the significant wave height, $H_s$, peak period, $T_p$, direction, etc.) and the wind profile (described by the mean wind speed, the spatial profile function, intensity, etc.).

Therefore, the sigma points, $\boldsymbol{x}_{n,i}$, ($i = 0,\ 1,\ 2,\ \ldots,\ 2\mathrm{N}$) to be used at the $n$-th update are calculated based on the $(n-1)$-th updated state as follows:

$$\boldsymbol{x}_{n,0} = \boldsymbol{X}_{n-1} \tag{1}$$

$$\boldsymbol{x}_{n,i} = \begin{cases} \boldsymbol{X}_{n-1} + \sqrt{[(\mathrm{N}+\lambda)\boldsymbol{P}_{n-1}]_i}, & i = 1,2,\ldots,N \\ \boldsymbol{X}_{n-1} - \sqrt{[(\mathrm{N}+\lambda)\boldsymbol{P}_{n-1}]_{i-\mathrm{N}}}, & i = N+1,\ldots,2N \end{cases} \tag{2}$$

$$\boldsymbol{x}_n = [\boldsymbol{x}_{n,0}, \boldsymbol{x}_{n,1}, \ldots, \boldsymbol{x}_{n,2\mathrm{N}}] \tag{3}$$

where N is the dimension of the system state vector. $\sqrt{[(\mathrm{N}+\lambda)\boldsymbol{P}_{n-1}]_i}$ represents the $i$-th column (or row) of the square root of the matrix $(\mathrm{N}+\lambda)\boldsymbol{P}_{n-1}$. The dimension of $\boldsymbol{x}_n$ is $\mathrm{N} \times (2\mathrm{N}+1)$. The coefficient $\lambda$ is computed by:

$$\lambda = \alpha^2(\mathrm{N}+\kappa) - \mathrm{N} \quad \alpha \in [0,1] \tag{4}$$

where $\alpha$ is the scaling factor, and $\kappa$ represents the scaling parameter, which is typically set to $3 - \mathrm{N}$ or 0.

The weights corresponding to the sigma points are independent of the update step which can be computed by:

$$\gamma_0^m = \frac{\lambda}{\lambda+\mathrm{N}} \tag{5}$$

$$\gamma_0^c = \frac{\lambda}{\lambda+\mathrm{N}} + 1 - \alpha^2 + \beta \tag{6}$$

$$\gamma_i^c = \gamma_i^m = \frac{\lambda}{2\lambda+\mathrm{N}}, \mathrm{i} = 1,2,\ldots,2\mathrm{N} \tag{7}$$

where $\gamma^m$ is the weight factor used for the state mean computation, while $\gamma^c$ is the weight factor used for the state covariance matrix computation. The subscription i indicates the $i$-th sigma point. $\beta$ was introduced by Julier to incorporate higher-order statistical information into the UKF [34]. For the Gaussian-distributed variables, $\beta$ is set to 2. It is recommended to ensure that the covariance matrix remains semi-positive definite [35]. All weight factors $\gamma_i^c$ must be non-negative, and the following conditions must hold: (1) $\kappa > -\mathrm{N}$, (2) $\alpha > \sqrt{\frac{\mathrm{N}}{4(\mathrm{N}+\kappa)}}$, where $\alpha$ is typically a small value.

### *2.2. State Propagation*

The state $(\boldsymbol{X}_{n-1}, \boldsymbol{P}_{n-1})$ is propagated by assuming that the key structural parameters remain approximately unchanged from the $(n-1)$-th to the $n$-th sea condition, i.e.,

$$\widehat{\boldsymbol{X}}_n = \boldsymbol{X}_{n-1} + \boldsymbol{W}_n \tag{8}$$

where $n$ represents the index for different sea conditions, $\widehat{\boldsymbol{X}}_n$ represents the possible value of the state vector after state propagation at the $n$-th sea condition. $\boldsymbol{W}_n \sim \mathcal{N}(0, \boldsymbol{Q}_n)$ is the process noise, assumed to follow Gaussian white noise distributions, representing state uncertainty among different sea conditions. $\boldsymbol{Q}_n$ is the process noise covariance at the $n$-th sea condition.

Therefore, the propagated state at the n-th sea condition can be calculated by:

$$\boldsymbol{X}_n^- = \boldsymbol{X}_{n-1} \tag{9}$$

$$\boldsymbol{P}_n^- = \boldsymbol{P}_{n-1} + \boldsymbol{Q}_n \tag{10}$$

where $(\boldsymbol{X}_n^-, \boldsymbol{P}_n^-)$ is the predicted state after propagation at the $n$-th sea condition.

### 2.3. Measurement Update

At the stage of measurement update, the observation space $\boldsymbol{Z}$ should be established. The parameters considered in $\boldsymbol{Z}$ should be highly relevant to the state space $\boldsymbol{X}$, i.e.,

$$\boldsymbol{Z} = h(\boldsymbol{X}) + \boldsymbol{V} \tag{11}$$

where $\boldsymbol{V} \sim \mathcal{N}(0, \boldsymbol{R})$ is the observation noise, following a Gaussian white noise distribution, $\boldsymbol{R}$ is the measurement uncertainty covariance. $h(\cdot)$ represents the function between $\boldsymbol{Z}$ and $\boldsymbol{X}$, which can be nonlinear.

At the $n$-th update, the residuals between the predicted modal parameters (based on $\boldsymbol{x}_n$ and the corresponding coupled simulation results) and the estimated modal parameters (based on the measured acceleration records $\mathrm{g}_{j,n}(\mathrm{t})^{measure}$) are considered to form the predicted observation space. The aim of the update is to make such residuals approach 0. $\mathrm{g}_{j,n}(\mathrm{t})$ represents the acceleration records at location $j$ along the turbine tower, $j = 1, 2, \ldots, J$. The modal parameters of OWTs, including the natural frequency $f_n$ and mode shape $\boldsymbol{\Phi}_n$, are computed based on $\mathrm{g}_{j,n}(\mathrm{t})$, $j = 1, 2, \ldots, J$, according to the covariance-driven stochastic subspace identification (COV-SSI) method [36].

In detail, the predicted modal parameters are calculated for each sigma point $\boldsymbol{x}_{n,i}$. First, the coupled dynamic simulation of OWTs (e.g., by OpenFAST [37]) should be conducted according to $\boldsymbol{x}_{n,i}$ and the operational status. The tower accelerations at $J$ locations are extracted, followed by a modal parameter identification according to COV-SSI, in order to obtain the predicted modal parameters for $\boldsymbol{x}_{n,i}$, denoted as $\overline{f}_{n,i}^{l}$ and $\overline{\boldsymbol{\Phi}}_{n,i}^{l}$, where $l \in \{1, 2, \ldots\}$ represents the order of the structural mode. It is worth mentioning that the modal parameters could be considered less dependent on the environmental conditions [36]. Therefore, the predicted values of the modal parameters are considered to be only influenced by the operational condition (normal operation or shutdown) and the uncertainty of the key structural parameters.

The measured tower accelerations $\mathrm{g}_{j,n}(\mathrm{t})^{true}$ for the n-th sea condition during the wind turbine's operation are applied to COV-SSI to estimate the modal parameters ($\overset{\sim}{f}_n^{l}$ and $\overset{\sim}{\boldsymbol{\Phi}}_n^{l}$, $l \in \{1, 2, \ldots\}$) accordingly, which are named as the measured modal parameters. The relative error $\boldsymbol{y}_{n,i}^{-}$ between the measured and predicted modal parameters based on $\boldsymbol{x}_{n,i}$ ($i = 0,\ 1,\ 2,\ \ldots,\ 2\mathrm{N}$), is further calculated using the following equations:

$$e_{f_{n,i}}^{l} = \frac{\left| \overline{f}_{n,i}^{l} - \overset{\sim}{f}_n^{l} \right|}{\overset{\sim}{f}_n^{l}} \tag{12}$$

$$\mathrm{e}_{\boldsymbol{\Phi}_{n,i}}^{l} = 1 - \mathrm{MAC}_{n,i}^{l} \tag{13}$$

$$\mathrm{MAC}_{n,i}^{l} = \frac{\left| \overline{\boldsymbol{\Phi}}_{n,i}^{l\ T} \cdot \overset{\sim}{\boldsymbol{\Phi}}_n^{l} \right|^2}{\left| \overline{\boldsymbol{\Phi}}_{n,i}^{l\ T} \cdot \overline{\boldsymbol{\Phi}}_{n,i}^{l} \right| \times \left| \overset{\sim}{\boldsymbol{\Phi}}_n^{l\ T} \cdot \overset{\sim}{\boldsymbol{\Phi}}_n^{l} \right|} \tag{14}$$

$$\boldsymbol{y}_{n,i}^{-} = \left[ \sum_{l}^{L} \frac{\mu_1 e_{f_{n,i}}^{l} + \mu_2 e_{\boldsymbol{\Phi}_{n,i}}^{l}}{L} \right] \tag{15}$$

where $e_{f_{n,i}}^{l}$ and $e_{\Phi_{n,i}}^{l}$ represent the relative errors between the measured and predicted values of the $l$-th order natural frequency and mode shape under the $n$-th sea condition for $\boldsymbol{x}_{n,i}$, respectively. $L$ represents the total number of mode parameters, MAC is the modal

assurance criterion, representing the similarity between the measured $l$-th order mode shape and the predicted one according to $\boldsymbol{x}_{n,i}$ under the $n$-th sea condition, on a scale from 0 to 1. $\mu_1$ and $\mu_2$ are the weights for combining the relative errors of the natural frequency and the mode shape, which are set to be 5/6 and 1/6, respectively [20]. The residual $\boldsymbol{y}_n^-$ represents the error of modal parameters between predicted and measured, which becomes a vector with a length of 1. Such residual preferably approaches 0, i.e., $\boldsymbol{Z}_n = 0$.

The predicted measurement mean for the $n$-th sea condition, considering all sigma points, is calculated as follows:

$$\widehat{\boldsymbol{Z}}_n = \sum_{i=0}^{2\mathrm{N}} \gamma_i^m \boldsymbol{y}_{n,i}^- \tag{16}$$

The covariance matrix of the predicted measurement value for the $n$-th sea condition is calculated as:

$$\boldsymbol{P}_{ZZ,n} = \sum_{i=0}^{2\mathrm{N}} \gamma_i^c (\boldsymbol{y}_{n,i}^- - \widehat{\boldsymbol{Z}}_n)(\boldsymbol{y}_{n,i}^- - \widehat{\boldsymbol{Z}}_n)^T + \boldsymbol{R}_n \tag{17}$$

where $\boldsymbol{R}_n$ denotes the measurement noise and the uncertainty in the measurement function, which may be related to the measurement sensors and sea conditions. The cross-covariance matrix between the state and the observation spaces for the $n$-th sea condition is calculated as follows:

$$\boldsymbol{P}_{XZ,n} = \sum_{i=0}^{2\mathrm{N}} \gamma_i^c (\boldsymbol{x}_{n,i} - \boldsymbol{X}_n^-)(\boldsymbol{y}_{n,i}^- - \widehat{\boldsymbol{Z}}_n)^T \tag{18}$$

The Kalman gain matrix is calculated by:

$$\boldsymbol{K}_n = \boldsymbol{P}_{XZ,n} \boldsymbol{P}_{ZZ,n}^{-1} \tag{19}$$

The mean and covariance of the state for the $n$-th sea condition are then updated using the observations and the Kalman gain matrix as follows:

$$\boldsymbol{X}_n = \boldsymbol{X}_n^- + \boldsymbol{K}_n(\boldsymbol{Z}_n - \widehat{\boldsymbol{Z}}_n) \tag{20}$$

$$\boldsymbol{P}_n = \boldsymbol{P}_n^- + \boldsymbol{K}_n \boldsymbol{P}_{ZZ,n} \boldsymbol{K}_n^T \tag{21}$$

The above describes a complete cycle for recursively updating the unknown key structural parameters $\boldsymbol{X}$ and their uncertainty about the OWT in operation. It is noted that the state space might not be constant throughout the whole project life over a period of decades. This method could continuously update the state space based on the new measurements and thus captures such value variation in the state space due to long-term effects such as aging. The proposed parameter update method for OWTs is based solely on the output measurement data and the coupled numerical model based on prior knowledge. The method first uses the COV-SSI method to extract the modal parameters of the structure from the measured data. Then, based on the UKF recursive Bayesian framework, it achieves more efficient updates of the physical parameters under the operational state of the structure. Compared to the traditional time-step-based UKF parameter update process, this study could make the update less computationally expensive, leading to potential real-time updating and making it more suitable for engineering applications.

## 3. Case Study Description

### *3.1. Numerical Model of the Jacket OWT*

A fully coupled numerical model of a jacket-type OWT was developed using FAST v8 [37], enabling simulation of the turbine's dynamic response under realistic operating conditions. The wind turbine system is based on the DTU 10 MW reference model developed

by the Technical University of Denmark [38]. The design of the tower and jacket support structure is based on previous studies [39]. The preliminary structural parameters are summarized in Table 1. The preliminary properties of the jacket-type OWT are illustrated in Figure 2. Accelerometers were assumed to be installed at five locations noted as locations A1–A5.

**Table 1.** The preliminary properties of the jacket-type OWT.

| Dimensions/Properties | Values |
|---|---|
| Hub mass | 105,520 kg |
| Wind turbine mass | 446,036 kg |
| Three blades mass | 125,196 kg |
| Tower height | 85.48 m |
| Tower top diameter and thickness | 5.5 m, 0.02 m |
| Tower base diameter and thickness | 7.57 m, 0.034 m |
| Rotor and hub diameter | 178.30 m, 5.60 m |
| Jacket height | 91.15 m |
| Cut-in, rated, cut-out wind speed | 4.0 m/s, 11.4 m/s, 25.0 m/s |
| Cut-in, rated rotor speed | 6.0 rpm, 9.0 rpm |
| Elastic modulus of steel | 210 GPa |
| Shear modulus of steel | 80.8 GPa |
| Density of steel | 8500 kg/m$^3$ |
| Poisson's ratio of steel | 0.3 |

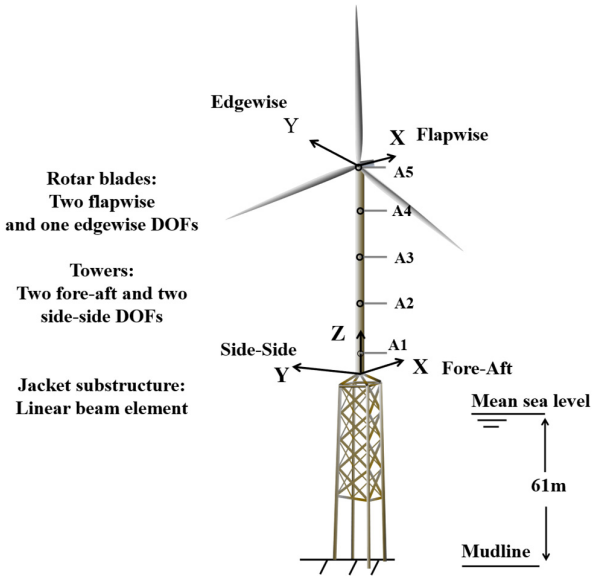



**Figure 2.** An illustration of the studied jacket-type OWT.

For the developed model, the rotor–nacelle assembly (RNA), consisting of the blades, nacelle, hub, and drivetrain, was modeled in the ElastoDyn module. The blades include the first two flapwise modes and the first edgewise mode, while the nacelle has two degrees of freedom (yaw and pitch). The first and second flapwise mode damping ratios were set to 3.0% and 8.4%, respectively, while the first edgewise mode damping ratio was set to 3.0%. The tower was modeled as a variable cross-section beam element, considering the first two as fore–aft (FA) and side-to-side (SS) modes, each with a damping ratio of 1% [40]. FA refers to the fore–aft direction, i.e., in line with the wind direction under the operational conditions. SS refers to the side-to-side direction, which is perpendicular to the FA direction. The first two orders of the blade and tower mode shapes were computed using BModes (v3.00) [41] and imported into ElastoDyn (v1.01).

The jacket substructure and transition piece were modeled in SubDyn (v1.01) based on the linear finite element beam theory. SubDyn applies the Craig–Bampton (C–B) method to reduce the degrees of freedom, with the retained internal modes assigned a damping ratio of 1%. The OWT was assumed to be rigidly fixed to the seabed.

The aerodynamic loads on the blades and tower are computed in AeroDyn (v14.04) using the blade element momentum (BEM) method [42], while the hydrodynamic loads on the foundation were calculated in HydroDyn (v2.03) using the Morison equation, accounting for both inertia and drag forces [43].

The turbulent wind fields were generated in TurbSim (v2.00) [43,44], following the IEC Kaimal spectrum model (Class B). Figure 3 presents a 3D visualization of the simulated turbulence, illustrating its random statistical characteristics. The simulation duration was set to be 1000 s, with a mean wind speed of 11.4 m/s and a turbulence intensity of 17.32%, among a horizontal width of 200 m, at the hub height of 119 m. The simulated wind field was fed into the InflowWind module of FAST, with the wind direction aligned to the turbine's FA axis.

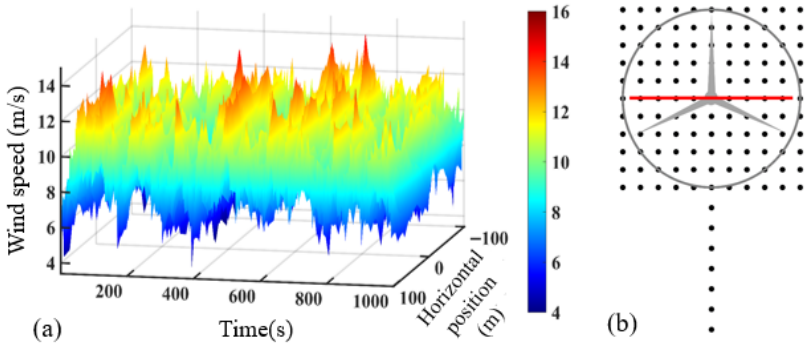



**Figure 3.** (**a**) The 3D turbulent wind map at a turbulence level of 17.32% simulated by Turbsim, and (**b**) a schematic diagram of the discrete wind field of the OWT.

### *3.2. Initial Model Analysis*

This study applies the proposed structural parameter identification method to the described numerical model of a 10 MW jacket-type offshore wind turbine. Many previous studies have taken the elastic modulus of materials as a primary damage identification parameter [30,45]. As a critical parameter, the elastic modulus directly influences both stiffness and dynamic response. The prior assumption for the elastic modulus is set to 180 GPa, whereas the actual value was considered to be 210 GPa. During identification, the model frequencies and mode shapes estimated by COV-SSI corresponding to each sea condition were used for creating measurement space as shown in Equations (12)–(15). The observation space was constructed using the relative error between the predicted and measured modal parameters.

A sensitivity analysis of the structural fundamental frequency was performed, as shown in Figure 4. The results reveal a strong positive correlation between the elastic modulus and the fundamental frequency. As the elastic modulus increases, the fundamental frequency rises correspondingly. Therefore, the first FA natural frequency and mode shape were used to build the measurement space, i.e., $L = 1$. For variations in the elastic modulus in the range of 180–400 GPa, the corresponding fundamental frequency changes from 0.20 Hz to 0.34 Hz, covering the baseline model's first-order natural frequency. This correlation indicates that, when the elastic modulus is unknown, its true value can be effectively inferred from the measured modal parameters.

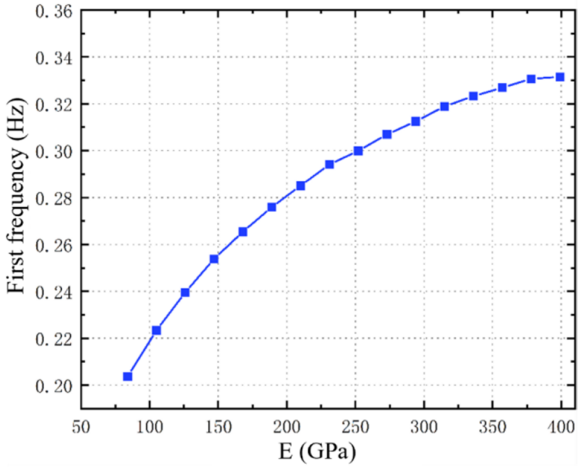



**Figure 4.** The sensitivity between the first-order natural frequency and the elastic modulus of the tower.

Free-decay simulations further show that the FA-direction fundamental frequency differs between parked and operational conditions, being 0.285 Hz and 0.292 Hz, respectively. Based on this, the tower's unknown elastic modulus is identified separately for parked and operational cases. Nine reliable modal parameter estimates, obtained from COV-SSI under various sea conditions, are randomly selected as measurement inputs. Since COV-SSI identifies the modal parameters using only output measurements, the actual sea conditions information is not emphasized in this section.

## 4. Numerical Validation

### *4.1. Results by the Sea-Condition-Based UKF Method*

The results of the structural parameter identification using the sea-condition-based UKF method are presented and discussed in this section. The observed and predicted measurement values of the structure under different sea conditions during the parked condition are shown in Figure 5. The updates of the tower's elastic modulus and its uncertainty are shown in Figure 6. The predicted values represent the updated elastic modulus after observations from each sea condition. The gray area (±2σ) represents the corresponding 95% confidence interval, where σ is the standard deviation of the variable. The update process gradually refines the elastic modulus and uncertainty of the structure through the observed values under sea conditions 1–9.

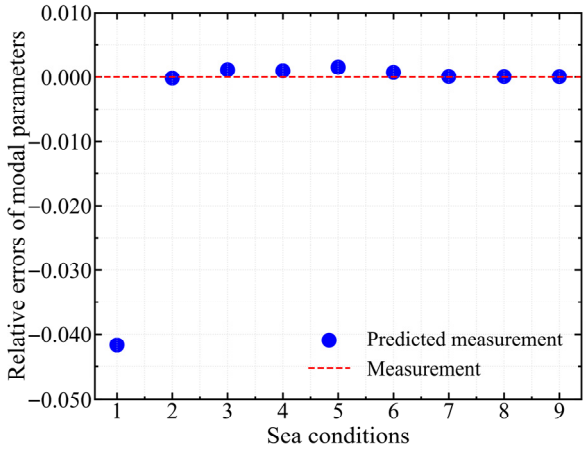



**Figure 5.** The values of $\bar{y}_{n,i}$ under parked conditions for each sea condition.

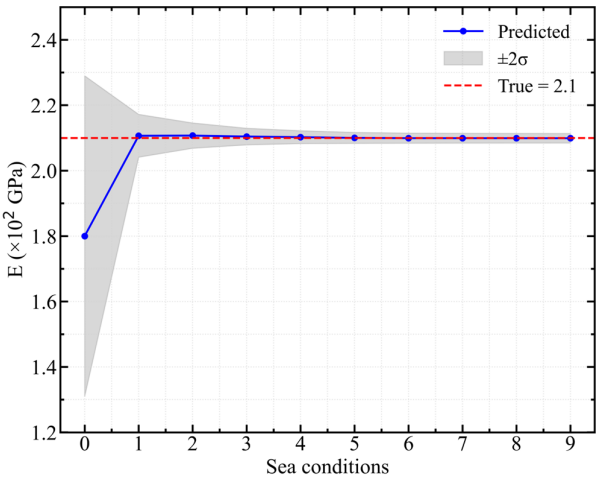
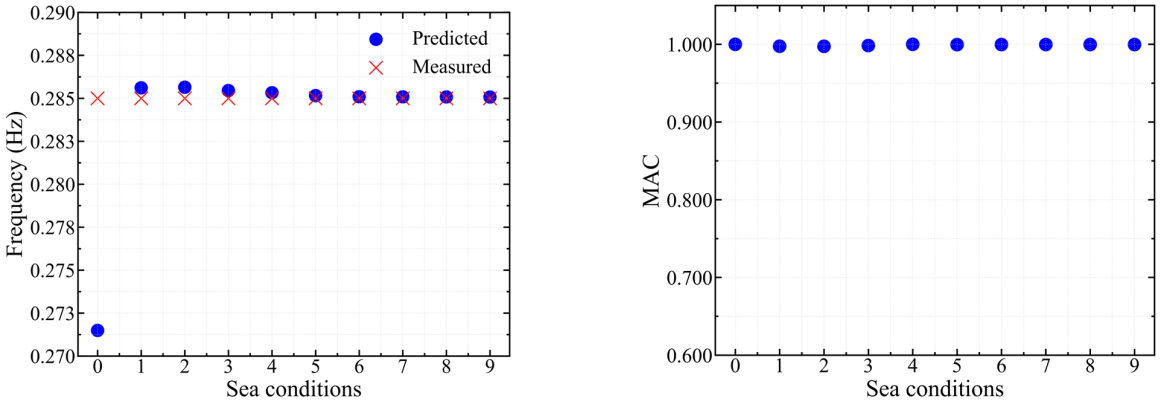



**Figure 6.** The update results of the tower's elastic modulus ($E$) under parked conditions.

Based on the initial model proposed in Section 3.2, the relative error between the prior value of the elastic modulus and the true value was 14.3% in sea condition 0. The initial state had a high level of uncertainty, with the initial uncertainty σ set at 24.5 GPa. As shown in Figure 6, the updated elastic modulus rapidly increased with changes in sea conditions. It reached a converged state (210.7 GPa) in sea condition 1. It gradually approached 210 GPa as the number of sea conditions increased. Additionally, the uncertainty in the parameter estimations decreased steadily and eventually stabilized. Furthermore, during this process, the value of $\boldsymbol{y}_{n,i}^{-}$ for sea condition 1 was −4.17%. After updating with one sea condition, it approached 0. As more sea conditions were observed, the value of $\boldsymbol{y}_{n,i}^{-}$ was gradually consistent with the actual measurement, i.e., 0.

Figure 7 shows a comparison between the predicted and actual structural modal parameters for each sea condition. Also, the initial structural fundamental frequency deviated significantly from the true value. After the update process, the predicted fundamental frequency approached the true value and gradually converged. Meanwhile, the MAC value for the mode shapes remained close to 1 for each sea condition. It indicated that the mode shape is not sensitive to the overall stiffness of the tower, compared to the fundamental frequency. Therefore, it is reasonable to assign weights to the errors in fundamental frequencies and mode shapes within Equation (15).




(**a**) Updated first-order frequency (**b**) Updated MAC (Modal Assurance Criterion)

**Figure 7.** The comparison between the predicted and measured values of the structural modal parameters under parked conditions: (**a**) the fundamental frequency and (**b**) MAC.

The verification results demonstrated that the improved UKF method enables the fast and accurate identification of the elastic modulus of the wind turbine tower under parked conditions.

Figures 8 and 9, respectively, show the values of $\boldsymbol{y}_{n,i}^{-}$ under different sea conditions, and the updated results of the wind turbine tower's elastic modulus under operating conditions. During the update process, the initial values for the elastic modulus and its uncertainty (standard deviation) were assumed to be 180 GPa and 24.5 GPa, respectively. The figures demonstrated that the estimated elastic modulus converged rapidly as sea conditions changed. At sea condition 2, the estimated elastic modulus was already close to the true value. As the number of observed sea conditions increased further, the elastic modulus eventually converged to 209.2 GPa. It caused a relative error of only 0.38% compared to the theoretical value. At the same time, the uncertainty of the parameter decreased from 24.5 GPa to 1 GPa. During this process, the values of $\boldsymbol{y}_{n,i}^{-}$ gradually approach the actual measured values.

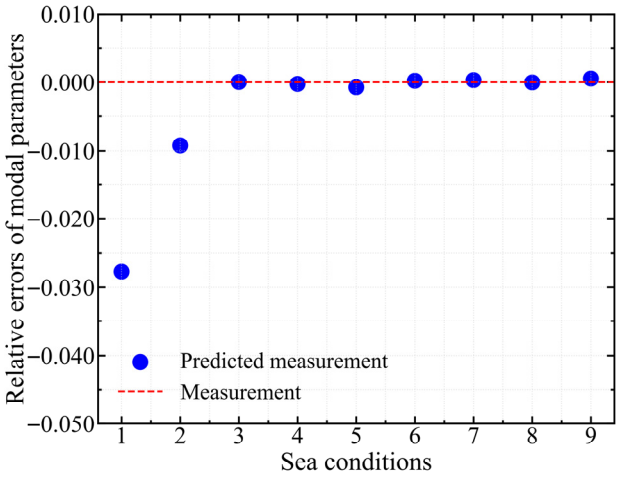



**Figure 8.** The values of $\boldsymbol{y}_{n,i}^{-}$ in the update under operating conditions for each sea condition.

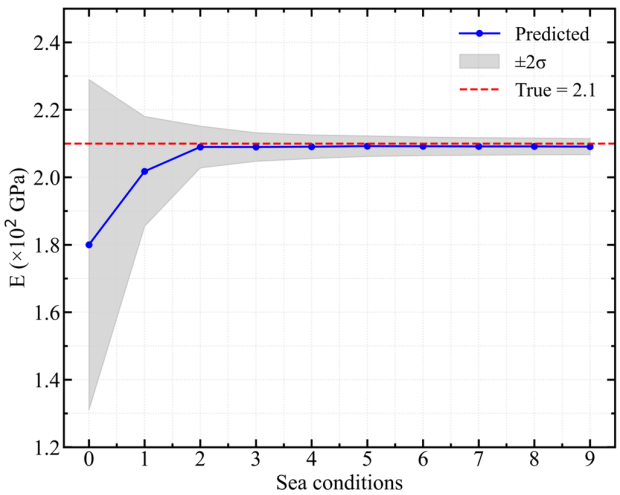



**Figure 9.** The update results of the tower's elastic modulus ($E$) under operating conditions.

By comparing the validation results under both the parked and operational states, it is evident that the improved UKF method demonstrates excellent convergence in the identification of key physical parameters. This method can quickly estimate the true values of the structure within a limited number of iterations. It can also achieve high accuracy (with a relative error of less than 0.5%) and significantly reduce fluctuations. The results

show a clear advantage in numerical stability. Therefore, this method is of great value for a real-time status update and evaluation in OWT structural health monitoring applications.

### *4.2. Structural Parameter Identification Using the Time-Step-Based UKF Method*

The traditional time-step-based updating methods typically use the structural response time histories (such as acceleration and displacement) to establish the observation space for updating the unknown parameters of the structure [28,46]. This section attempts to update the tower's elastic modulus based on the tower's acceleration response time history. It used acceleration responses measured at three positions on the tower: #A2, #A4, and #A5, as shown in Figure 2. The response sampling frequency was 20 Hz, and the time segment was from 50 s to 60 s.

Three load conditions (LCs) were considered, i.e., the parked condition (LC1: $H_s$ = 2.5 m, $T_p$ = 6.5 s), the rated wind speed with unstable blade operation condition (LC2: $H_s$ = 2.5 m, $T_p$ = 6.5 s, wind speed = 11.4 m/s), and the high wind speed with stable blade operation condition (LC3: $H_s$ = 2.5 m, $T_p$ = 6.5 s, wind speed = 15.0 m/s). The time-step-based updating method updates the structural parameters at each time step. The true elastic modulus of the tower was 210 GPa. Moreover, the initial tower material elastic modulus was considered to be 180 GPa. The time-step-based UKF updating method demonstrated good convergence under all three typical conditions. The updated results for LC1 are shown in Figure 10 as an example. In LC1, the identification result converged to the true value after approximately 300 time steps.

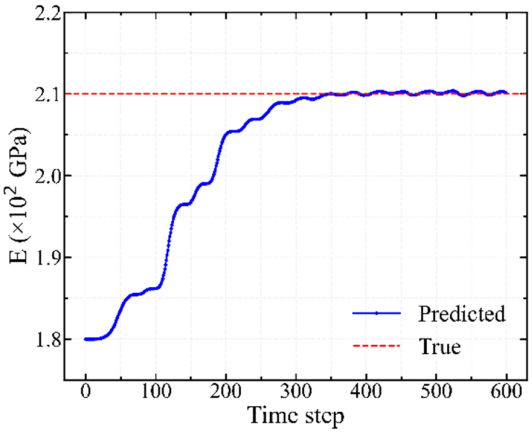



**Figure 10.** The parameter identification based on the time-step response for LC1.

Compared to the time-step-based structural parameter identification method, the sea-condition-based method has an evident advantage in convergence speed and stability. Under the parked condition, the elastic modulus began to update to approach the true value (210 GPa) after only about 15 s. It required approximately 300 time steps to reach a stable state. In contrast, the sea-condition-based updating method can converge to the true value much faster (e.g., under the parked condition, it converged after just one sea condition).

It is important to acknowledge that the time-step-based updating method has several limitations in practical engineering applications: (1) it requires prior knowledge of the load information, and (2) the measurements of structural responses demand precise time synchronization. These requirements are often difficult to meet in practice. Moreover, the measurement noise can significantly affect the parameter identification accuracy. Although existing studies have proposed an improved UKF method for identifying structural parameters that are synchronized with the load, these methods are mainly limited to identification under single load excitation conditions and are typically verified through numerical simu-

lations or simple frame structure experiments [28]. This limitation makes them difficult to apply to offshore wind turbine structures, which are subjected to complex loads.

In contrast, the improved sea-condition-based UKF updating method has distinct advantages. This method relies solely on the output measurement data and does not have strict requirements for the input load information. The time spent on the one-step update was recorded. The time-step-based updating method used several minutes to complete one update corresponding to a time step of 0.05 s. In comparison, the updating based on the sea-condition-based method was completed in about half an hour. It must be emphasized that the presented updating speed (i.e., the time spent on one update) should be treated more qualitatively and relatively because the tested programs, the numerical modeling, and the applied simulation solver could be subject to essential optimization in terms of computational efficiency. More importantly, the sea-condition-based updating demonstrates an excellent convergence rate to the real value in only 1–2 steps, while it took about 400 steps to converge by the time-step-based method. For the new method, the updating time spent toward convergence is essentially less than that of the traditional one. In summary, the new method was demonstrated with excellent stability and efficiency during the updating process.

## 5. Validation by Scaled Experiment

This section validates the proposed key parameter identification framework using the experimental data from a 1:75 scaled model of a jacket-type OWT [39,47]. The aim is to experimentally verify the effectiveness of the proposed identification method and assess its applicability in real engineering applications. The results will provide valuable technical insights for the practical application of digital twin technology in offshore wind energy.

### *5.1. Experimental Overview*

The experimental work was conducted by the research team in earlier stages, and the scale model was based on the DTU 10 MW benchmark model from the Technical University of Denmark (DTU) [38].

The supporting structure used a typical jacket foundation design, with the geometric parameters strictly adhering to real-world marine environmental conditions. The top and bottom widths of the jacket were 12.00 m and 15.00 m, respectively, and the jacket height was 70.15 m. The scale factor of the prototype wind turbine was calculated based on the structural elastic similarity, the aerodynamic similarity, and the hydrodynamic similarity theory, as shown in Table 2. The final design of the scaled model is shown in Figure 11.

**Table 2.** The similarity between the test model and the prototype.

| Value | Dimension | Similarity Relationship | Scale Ratio |
|---|---|---|---|
| Length | $[\mathrm{L}]$ | $\lambda_{\mathrm{L}}$ | 0.013 |
| Density | $\left[\mathrm{ML}^{-3}\right]$ | $\lambda_{\rho}=1$ | 1.00 |
| Mass | $[\mathrm{M}]$ | $\lambda_{\mathrm{L}}^{3}$ | $2.4\times10^{-6}$ |
| Velocity | $\left[\mathrm{LT}^{-1}\right]$ | $\sqrt{\lambda_{\mathrm{L}}}$ | 0.11 |
| Acceleration | $\left[\mathrm{LT}^{-2}\right]$ | $\lambda_{\mathrm{g}}=1$ | 1.00 |
| rotor speed | $\left[\frac{1}{\mathrm{T}}\right]$ | $\lambda_{\Omega}$ | 8.66 |
| Time | $[\mathrm{T}]$ | $\sqrt{\lambda_{\mathrm{L}}}$ | 0.11 |
| Frequency | $\left[\frac{1}{\mathrm{T}}\right]$ | $\frac{1}{\sqrt{\lambda_{\mathrm{L}}}}$ | 8.66 |
| Force | $\left[\mathrm{MLT}^{-2}\right]$ | $\lambda_{\mathrm{L}}^{3}$ | $2.4\times10^{-6}$ |

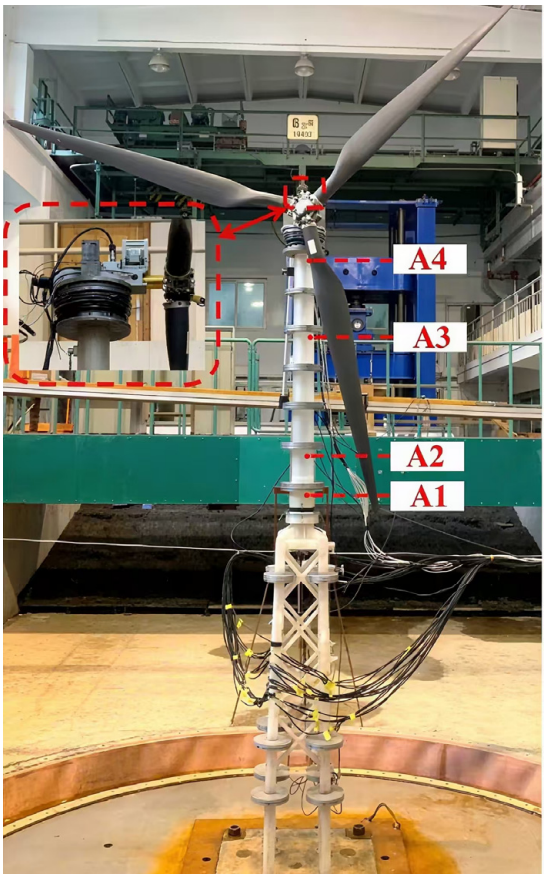



**Figure 11.** An illustration of the experimental setup.

Accelerometers were installed at four locations on the device: #A1, #A2, #A3, and #A4. These sensors recorded the tower's acceleration in the horizontal downwind direction (FA). The sampling frequency was established at 512 Hz, and the duration of the acceleration records was 330 s. This study concentrates on the first two modal frequencies in the FA direction. It used acceleration data in the FA direction as the input parameter for subsequent algorithms. To enhance computational efficiency, the signal sampling frequency of 512 Hz was downsampled to 128 Hz.

During the initial start-up phase of the wind turbine, the structure exhibited instability. The acceleration responses were highly fluctuating. To avoid the influence of these fluctuations on the identification method, only acceleration data from 50 s to 300 s were used for modal parameter identification. Additionally, a free decay test on the model was conducted to measure the top acceleration's free decay curve. The fast Fourier transform analysis of the decay curve revealed a structural fundamental frequency of 2.87 Hz [47], which was used as the true reference value for validation.

In this study, six different operating conditions were selected for the experiments. Each condition was tested twice to ensure the reliability and consistency of the results. The detailed parameters of the conditions before and after scaling are shown in Tables 3 and 4. The conditions were defined as follows:

**Table 3.** The prototype conditions (pre-scaling).

| Case No. | Description | Wind Speed (m/s) | Blade Pitch (deg) | Rotor Speed (rpm) | Water Depth (m) | Wave Height (m) | Wave Period (s) |
|---|---|---|---|---|---|---|---|
| LC1 | - | - | 0.0 | 0.0 | 61.0 | 1.50 | 9.0 |
| LC2 | - | - | 0.0 | 0.0 | | 3.00 | 10.0 |
| LC3 | Steady wind and regular wave | 6.0 | 0.9 | 6.00 | | - | - |
| LC4 | Steady wind and regular wave | 11.4 | 0.0 | 9.60 | | - | - |
| LC5 | Steady wind and regular wave | 6.0 | 0.9 | 6.00 | | 1.50 | 9.0 |
| LC6 | Steady wind and regular wave | 11.4 | 0.0 | 9.60 | | 3.00 | 10.0 |

**Table 4.** The scaled test conditions (scale factor 1:75).

| Case No. | Description | Wind Speed (m/s) | Blade Pitch (deg) | Rotor Speed (rpm) | Water Depth (m) | Wave Height (m) | Wave Period (s) |
|---|---|---|---|---|---|---|---|
| LC1 | - | - | 0.0 | 0.0 | 0.8 | 0.02 | 0.9 |
| LC2 | - | - | 0.0 | 0.0 | | 0.04 | 1.1 |
| LC3 | Steady wind and regular wave | 0.7 | 0.9 | 51.96 | | - | - |
| LC4 | Steady wind and regular wave | 1.3 | 0.0 | 83.14 | | - | - |
| LC5 | Steady wind and regular wave | 0.7 | 0.9 | 51.96 | | 0.02 | 0.9 |
| LC6 | Steady wind and regular wave | 1.3 | 0.0 | 83.14 | | 0.04 | 1.1 |

LC1 and LC2 described the parked conditions with regular wave action only, capturing the tower's response to waves in the absence of wind.

LC3 and LC4 illustrated the operating conditions under steady wind only, showing the turbine's behavior under constant wind loading without wave effects.

LC5 and LC6 represented the operating conditions with combined wind and wave action, reflecting realistic offshore scenarios where both forces act on the structure simultaneously.

### *5.2. Results of Modal Parameter Identification Using Scaled Model*

The input parameters for the COV-SSI method were selected based on the acceleration response time histories that were recorded under six different operating conditions. In the modal parameter identification process, the key hyperparameters for the method were set as follows: the natural frequency threshold between adjacent modes was not to exceed 0.1, the deviation of MAC was controlled within 0.1, and the damping ratio deviation limit was set to 50%. The model order was chosen to be within the range of 30–50 to ensure an accurate identification of the structural modal parameters. The structural fundamental frequency identification results for the six operating conditions are shown in Figure 12. The stability plot and clustering results for the LC5 are shown in Figures 13 and 14, respectively. In the stability plot, continuous stable axes are formed, each corresponding to the peak of the power spectral density of the acceleration response. The clustering results indicate that the 3P frequency (2.7 Hz) and the structural fundamental frequency (2.89 Hz) are accurately identified under LC5, demonstrating a high identification accuracy.

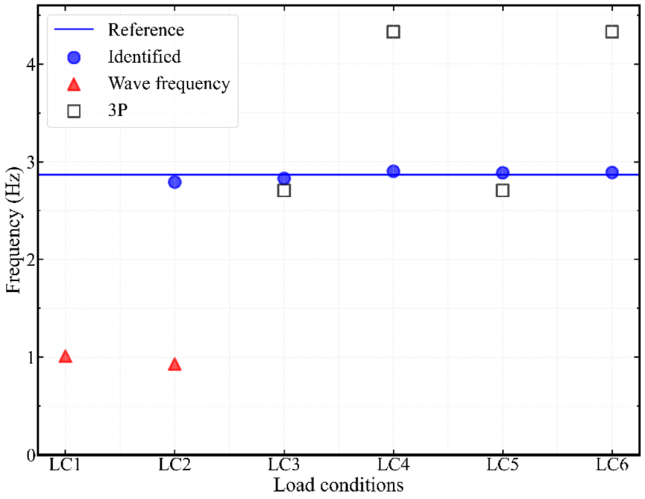



**Figure 12.** The results of the identified relevant critical frequencies in the scaled tests.

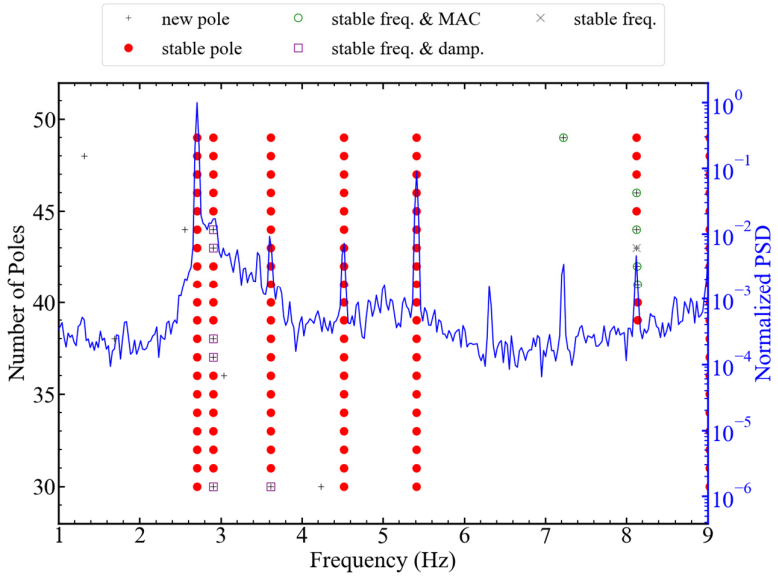



**Figure 13.** The stabilization plot of the modal identification under LC5.

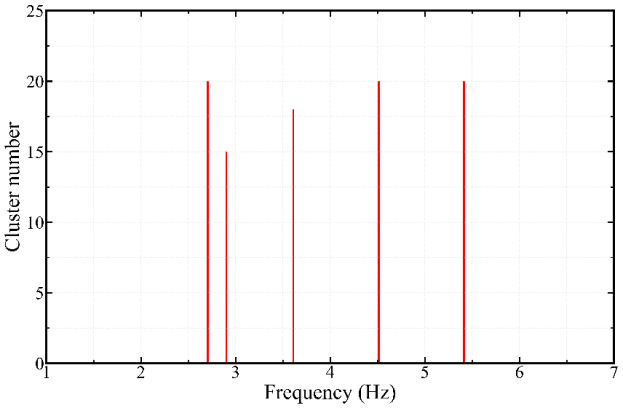



**Figure 14.** The clustering results for the stabilization plot of LC5.

### *5.3. Results of Physical Parameter Identification by Improved UKF Based on Experimental Data*

The improved UKF method was validated based on the experimental data. The modal parameter identification results from LC3-LC6 were used to establish the observation space for the parameter identification of the test tower's elastic modulus. The tower was made of

acrylic (PMMA, polymethyl methacrylate), with a material elastic modulus of 3.85 GPa. The equivalent elastic modulus of the tower was also 3.85 GPa, and the initial value of the elastic modulus was set to 3.55 GPa. Due to the limited experimental data, only the structural operating conditions were selected for the update, resulting in eight iterations of the tower's elastic modulus updates. The updates of the elastic modulus and uncertainty are shown in Figure 15. The update results show that the first two updates deviated from the true value, which was mainly due to the large modal parameter identification errors in LC3. However, subsequent updates converged rapidly and ultimately stabilized at 4.02 GPa, with a 4.2% identification error.

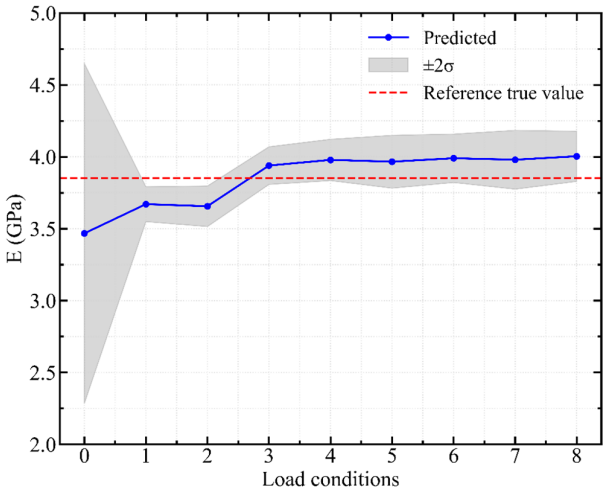



**Figure 15.** The update results of the tower's elastic modulus for the scaled test.

The experimental validation results indicate that the improved UKF framework demonstrates good parameter convergence, stable identification accuracy, and strong robustness to disturbances within a limited number of iterations. The stable identification errors observed in the final experimental update results are primarily attributed to modeling errors and measurement errors. Modeling errors may arise from simplifications in assumptions, uncertainties in material properties, and deviations in structural geometric parameters. Measurement errors, on the other hand, may arise from sensor accuracy, noise during the data acquisition process, and the influence of environmental factors. In the future, the value of engineering applications can be further enhanced by introducing more accurate finite element models, developing targeted noise reduction algorithms, improving uncertainty quantification methods, and integrating multi-source data.

## 6. Conclusions

The traditional time-step-based Bayesian updating methods suffer from high computational complexity and slow convergence, particularly when identifying parameters under the combined wind and wave loads. This study proposes a parameter identification method that integrates modal parameter identification with Bayesian recursive updating. A 10 MW jacket-type OWT is used for the method validation, through both numerical simulations and scaled-model experiments. The proposed sea-condition-based updating method does not strictly require knowing the input load information. Its feasibility and efficiency for structural parameter identification are also demonstrated to have significant engineering values.

The numerical validations indicate that the improved method can rapidly converge to the true values within a limited number of iterations. It demonstrates excellent stability and accuracy. The validation with experimental data shows that the relative error in the

identified elastic modulus of the tower is only 4.2%, proving the robustness of the method with noisy measurements and numerical modeling errors.

The proposed parameter identification method succeeded in identifying the elastic modulus of the test tower with a high convergence speed and accuracy. Future work could be focused on the investigation of method sensitivity to noise and sensor layout, measurement space design, and conducting in situ verifications. Beyond elastic modulus identification, the framework could be extended to update other critical parameters. It must be admitted that the capability of the proposed method in terms of handling more complicated state spaces has not yet been revealed. A design of multi-dimensional state and observation spaces and consequent algorithm modification is expected and of interest to perform in the future.

**Author Contributions:** Conceptualization, X.H. and C.Z.; methodology, X.H. and C.Z.; software, C.Z.; validation, Z.G., Q.L., W.W. and X.L.; formal analysis, X.H. and C.Z.; investigation, X.H., C.Z. and Z.G.; resources, X.H. and X.L.; data curation, C.Z. and W.W.; writing—original draft preparation, X.H., C.Z. and Z.G.; writing—review and editing, X.H., Z.G., W.W., Q.L. and X.L.; visualization, C.Z.; supervision, X.H. and X.L.; project administration, X.H. and W.W.; funding acquisition, X.L. All authors have read and agreed to the published version of the manuscript.

**Funding:** This research was partly funded by the Innovation Yongjiang 2035 Key Research and Development Programme, grant number 2025Z051.

**Data Availability Statement:** Data are contained within the article.

**Conflicts of Interest:** Chen Zhang is an employee of China Nuclear Power Engineering Co., Ltd. Qiang Liu is an employee of PowerChina Huadong Engineering Corporation Limited. The paper reflects the views of the scientists and not the companies.

## References

1. REN21. *Renewables 2023 Global Status Report*; REN21: Paris, France, 2023.
2. Han, X.; Leira, B.J.; Sævik, S. Vessel hydrodynamic model tuning by Discrete Bayesian updating using simulated onboard sensor data. *Ocean Eng.* **2021**, *220*, 108407. [CrossRef]
3. Hu, F.; Zhi, L.; Hu, Z.; Chen, B. Modal parameter identification of civil structures using symplectic geometry mode decomposition. *Wind Struct. Int. J.* **2023**, *36*, 61–73.
4. Devriendt, C.; Magalhães, F.; Weijtjens, W.; De Sitter, G.; Cunha, Á.; Guillaume, P. Structural health monitoring of offshore wind turbines using automated operational modal analysis. *Struct. Health Monit.* **2014**, *13*, 644–659. [CrossRef]
5. Zhou, L.; Li, Y.; Liu, F.; Jiang, Z.; Yu, Q.; Liu, L. Investigation of dynamic characteristics of a monopile wind turbine based on sea test. *Ocean Eng.* **2019**, *189*, 106308. [CrossRef]
6. Augustyn, D.; Smolka, U.; Tygesen, U.T.; Ulriksen, M.D.; Sørensen, J.D. Data-driven model updating of an offshore wind jacket substructure. *Appl. Ocean Res.* **2020**, *104*, 102366. [CrossRef]
7. Song, M.; Mehr, N.P.; Moaveni, B.; Hines, E.; Ebrahimian, H.; Bajric, A. One year monitoring of an offshore wind turbine: Variability of modal parameters to ambient and operational conditions. *Eng. Struct.* **2023**, *297*, 117022. [CrossRef]
8. Ozbek, M.; Meng, F.; Rixen, D.J. Challenges in testing and monitoring the in-operation vibration characteristics of wind turbines. *Mech. Syst. Signal Process.* **2013**, *41*, 649–666. [CrossRef]
9. Benedetti, M.; Fontanari, V.; Zonta, D. Structural health monitoring of wind towers: Remote damage detection using strain sensors. *Smart Mater. Struct.* **2011**, *20*, 055009. [CrossRef]
10. Cong, S.; Hu, S.-L.J.; Li, H.-J. Inverse modeling of damping and soil–structure interface for monopiled offshore wind turbines. *Ocean Eng.* **2020**, *216*, 108079. [CrossRef]
11. Han, X.; Sævik, S.; Leira, B.J. Tuning of vessel parameters including sea state dependent roll damping. *Ocean Eng.* **2021**, *233*, 109084. [CrossRef]
12. Kamariotis, A.; Chatzi, E.; Straub, D. A framework for quantifying the value of vibration-based structural health monitoring. *Mech. Syst. Signal Process.* **2023**, *184*, 109708. [CrossRef]
13. Ni, P.; Li, J.; Hao, H.; Han, Q.; Du, X. Probabilistic model updating via variational Bayesian inference and adaptive Gaussian process modeling. *Comput. Methods Appl. Mech. Eng.* **2021**, *383*, 113915. [CrossRef]

14. Ntotsios, E.; Papadimitriou, C.; Panetsos, P.; Karaiskos, G.; Perros, K.; Perdikaris, P.C. Bridge health monitoring system based on vibration measurements. *Bull. Earthq. Eng.* **2009**, *7*, 469–483. [CrossRef]
15. Lam, H.-F.; Yang, J.; Au, S.-K. Bayesian model updating of a coupled-slab system using field test data utilizing an enhanced Markov chain Monte Carlo simulation algorithm. *Eng. Struct.* **2015**, *102*, 144–155. [CrossRef]
16. Simoen, E.; De Roeck, G.; Lombaert, G. Dealing with uncertainty in model updating for damage assessment: A review. *Mech. Syst. Signal Process.* **2015**, *56*, 123–149. [CrossRef]
17. Song, M.; Renson, L.; Noël, J.P.; Moaveni, B.; Kerschen, G. Bayesian model updating of nonlinear systems using nonlinear normal modes. *Struct. Control Health Monit.* **2018**, *25*, e2258. [CrossRef]
18. Song, M.; Moaveni, B.; Papadimitriou, C.; Stavridis, A. Accounting for amplitude of excitation in model updating through a hierarchical Bayesian approach: Application to a two-story reinforced concrete building. *Mech. Syst. Signal Process.* **2019**, *123*, 68–83. [CrossRef]
19. Xu, P.; Chen, J.; Li, J.; Fan, S.; Xu, Q. Using Bayesian updating for monopile offshore wind turbines monitoring. *Ocean Eng.* **2023**, *280*, 114801. [CrossRef]
20. Moynihan, B.; Mehrjoo, A.; Moaveni, B.; McAdam, R.; Rüdinger, F.; Hines, E. System identification and finite element model updating of a 6 MW offshore wind turbine using vibrational response measurements. *Renew. Energy* **2023**, *219*, 119430. [CrossRef]
21. Chatzi, E.N.; Smyth, A.W. The unscented Kalman filter and particle filter methods for nonlinear structural system identification with non-collocated heterogeneous sensing. *Struct. Control Health Monit.* **2009**, *16*, 99–123. [CrossRef]
22. Azam, S.E.; Mariani, S. Dual estimation of partially observed nonlinear structural systems: A particle filter approach. *Mech. Res. Commun.* **2012**, *46*, 54–61. [CrossRef]
23. Wu, M.; Smyth, A.W. Application of the unscented Kalman filter for real-time nonlinear structural system identification. *Struct. Control Health Monit. Off. J. Int. Assoc. Struct. Control Monit. Eur. Assoc. Control Struct.* **2007**, *14*, 971–990. [CrossRef]
24. Ebrahimian, H.; Astroza, R.; Conte, J.P. Extended Kalman filter for material parameter estimation in nonlinear structural finite element models using direct differentiation method. *Earthq. Eng. Struct. Dyn.* **2015**, *44*, 1495–1522. [CrossRef]
25. Astroza, R.; Ebrahimian, H.; Conte, J.P. Material parameter identification in distributed plasticity FE models of frame-type structures using nonlinear stochastic filtering. *J. Eng. Mech.* **2015**, *141*, 04014149. [CrossRef]
26. Song, M.; Astroza, R.; Ebrahimian, H.; Moaveni, B.; Papadimitriou, C. Adaptive Kalman filters for nonlinear finite element model updating. *Mech. Syst. Signal Process.* **2020**, *143*, 106837. [CrossRef]
27. Erazo, K.; Moaveni, B.; Nagarajaiah, S. Bayesian seismic strong-motion response and damage estimation with application to a full-scale seven story shear wall structure. *Eng. Struct.* **2019**, *186*, 146–160. [CrossRef]
28. Li, X.; Zhang, C.; Zheng, Y.; Zhang, N. A novel constrained UKF method for both updating structural parameters and identifying excitations for nonlinear structures. *Soil Dyn. Earthq. Eng.* **2022**, *158*, 107291. [CrossRef]
29. Song, M.; Christensen, S.; Moaveni, B.; Brandt, A.; Hines, E. Joint parameter-input estimation for virtual sensing on an offshore platform using output-only measurements. *Mech. Syst. Signal Process.* **2022**, *170*, 108814. [CrossRef]
30. Song, M.; Moaveni, B.; Ebrahimian, H.; Hines, E.; Bajric, A. Joint parameter-input estimation for digital twinning of the Block Island wind turbine using output-only measurements. *Mech. Syst. Signal Process.* **2023**, *198*, 110425. [CrossRef]
31. Han, X.; Leira, B.J.; Sævik, S.; Ren, Z. Onboard tuning of vessel seakeeping model parameters and sea state characteristics. *Mar. Struct.* **2021**, *78*, 102998. [CrossRef]
32. Ma, C.; Ban, J.; Zi, G. Comparative study on the dynamic responses of monopile and jacket-supported offshore wind turbines considering the pile-soil interaction in transitional waters. *Ocean Eng.* **2024**, *292*, 116564. [CrossRef]
33. Yan, A.; Golinval, J.-C. Structural damage localization by combining flexibility and stiffness methods. *Eng. Struct.* **2005**, *27*, 1752–1761. [CrossRef]
34. Eric, A.W.; Van Der Merwe, R. The unscented Kalman filter for nonlinear estimation. In Proceedings of the IEEE 2000 Adaptive Systems for Signal Processing, Communications, and Control Symposium, Lake Louise, AB, Canada, 4 October 2000; pp. 153–158.
35. Julier, S.J. The scaled unscented transformation. In *2002 American Control Conference (IEEE Cat No CH37301)*; IEEE: New York, NY, USA, 2002.
36. Zhang, C.; Han, X.; Li, C.; Leira, B.J.; Sævik, S.; Lu, D.; Shi, W.; Li, X. Modal Parameter Identification of Jacket-Type Offshore Wind Turbines Under Operating Conditions. *J. Mar. Sci. Eng.* **2024**, *12*, 2083. [CrossRef]
37. Jonkman, B.; Jonkman, J.M. *FAST User's Guide: Version 8.16.00*; National Renewable Energy Laboratory: Golden, CO, USA, 2016.
38. Bak, C.; Zahle, F.; Bitsche, R.D.; Kim, T.; Yde, A.; Henriksen, L.C.; Hansen, M.H.; Blasques, J.P.A.A.; Gaunaa, M.; Natarajan, A. The DTU 10-MW Reference Wind Turbine. In Proceedings of the Danish Wind Power Research, Trinity, Denmark, 27–28 May 2013.
39. Lu, D.; Wang, W.; Li, X. Experimental study of structural vibration control of 10-MW jacket offshore wind turbines using tuned mass damper under wind and wave loads. *Ocean Eng.* **2023**, *288*, 116015. [CrossRef]
40. Damiani, R.; Jonkman, J.; Hayman, G. *SubDyn User's Guide and Theory Manual*; National Renewable Energy Laboratory: Golden, CO, USA, 2015.
41. Bird, G. *User's Guide to BModes*; National Renewable Energy Laboratory: Golden, CO, USA, 2005.

42. Moriarty, P.J.; Hansen, A.C. *AeroDyn Theory Manual*; National Renewable Energy Laboratory: Golden, CO, USA, 2005.
43. Jonkman, J.M.; Robertson, A.; Hayman, G.J. *HydroDyn User's Guide and Theory Manual*; National Renewable Energy Laboratory: Golden, CO, USA, 2005.
44. Jonkman, B. *TurbSim User's Guide v2. 00.00*; National Renew Energy Laboratory: Golden, CO, USA, 2014.
45. Guo, J.; Ji, X.; Song, H.; Chang, S.; Liu, F. Unsupervised statistical estimation of offshore wind turbine vibration for structural damage detection under varying environmental conditions. *Eng. Struct.* **2022**, *272*, 115005. [CrossRef]
46. Huang, J.; Li, D.; Zhang, C.; Li, H. Improved Kalman filter damage detection approach based on $l_p$ regularization. *Struct. Control Health Monit.* **2019**, *26*, e2424. [CrossRef]
47. Huan, C.; Lu, D.; Zhao, S.; Wang, W.; Shang, J.; Li, X.; Liu, Q. Experimental study of ultra-large jacket offshore wind turbine under different operational states based on joint aero-hydro-structural elastic similarities. *Front. Mar. Sci.* **2022**, *9*, 915591. [CrossRef]


**Disclaimer/Publisher's Note:** The statements, opinions and data contained in all publications are solely those of the individual author(s) and contributor(s) and not of MDPI and/or the editor(s). MDPI and/or the editor(s) disclaim responsibility for any injury to people or property resulting from any ideas, methods, instructions or products referred to in the content.